Nematic Conformation of Oxyethylene Spacers Involved in Main-Chain Liquid Crystals

Hidemine Furuya,[1] Hiroshi Iwanaga,[2] Takeshi Nakajima,[3] Akihiro Abe[4]*

[1]Tokyo Institute of Technology, Department of Organic and Polymeric Materials, 2-12-1 Ookayama, Meguro-ku, Tokyo 152-8552, Japan
[2]Fuji Photo Film Co. Ltd., Ashigara Research Laboratories, 210 Nakamura, Minamiashigara 250-0193, Japan
[3]SunAllomer Ltd., Kawasaki Development Center, 2-3-2 Yako, Kawasaki-ku, Kawasaki 210-8548, Japan
[4]Tokyo Institute of Polytechnics, Department of Applied Chemistry, 1583 Iiyama, Atsugi 243-0297, Japan

Summary: ^{2}HNMR measurements were performed on main-chain dimer and polymer liquid crystals (LC) having oxyethylene (OE) spacers -$(OCH_2CH_2)_xO$- (x=2, 3). The orientational as well as conformational characteristics of these molecules have been investigated in bulk and in a nematic solution. The OE spacer was found to take spatial arrangements characteristics of the nematic phase. The nematic conformation of the spacer remains nearly invariant over a wide range of temperature and concentration. In these analyses, the ratio of the deuterium quadrupolar splittings $\Delta\nu/\Delta\nu^R$ ($\Delta\nu$: spacer and $\Delta\nu^R$: mesogenic unit) provided an important information regarding the spatial configuration of molecules in the LC state. The results obtained in this study are consistent with our previous conclusion drawn on a series of main-chain LC oligomers and polymers comprising n-alkane spacers -$O(CH_2)_nO$- (n=9, 10).

Introduction

Flexible polymers often exhibit crystallization or liquid crystallization. In these first-order transitions, changes in the spatial arrangement of polymer chains are considered to be a major factor governing the transition entropy. Thermodynamic significance of the conformation entropy in these examples has been extensively studied on the basis of the rotational isomeric state (RIS) treatment.

In a series of papers,[1-8] we have reported the results of ^{2}HNMR and pressure-volume-temperature (*PVT*) studies of dimer and trimer liquid crystals (LC) having structures such as

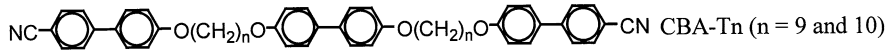

CBA-Tn (n = 9 and 10)

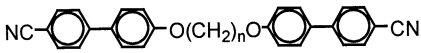

CBA-n (n = 9 and 10)

 CCC 1022-1360/00/$ 17,50+.50/0

where n designates the number of carbon atoms in the spacer. In these compounds, mesogenic cores (cyanobiphenyl groups) are linked with n-alkane spacers via the ether linkage. CBA-n and CBA-Tn exhibit two well-defined phase transitions as a function of temperature: crystal (C) - nematic LC (N) - isotropic melt (I). These ether-type LCs are known to exhibit a pronounced odd-even oscillation in various thermodynamic quantities at the NI phase boundaries,[9] indicating that the spatial configuration of the spacer plays a significant role.[10] The values of the constant-volume transition entropies $(\Delta S_{tr})_v$ derived from *PVT* studies were favorably compared with the conformational entropies of the spacer calculated from the spatial arrangements elucidated spectroscopically in the two relevant states.[3]

The results of the ^{2}HNMR analysis on these dimer and trimer LCs may be summarized as follows: (1) Under a uniaxial potential field, both spacer and mesogenic units at the terminals tend to align along the domain axis. Consequently the individual mesogenic cores inevitably incline to some extent with respect to the direction of molecular extension, giving rise to a moderate value of the orientational order parameter of mesogenic cores.[6] (2) While the orientational fluctuation of the entire molecule varies as a function of temperature, the nematic conformation of the spacer remain nearly invariant over the entire range of the LC state.[3,6] (3) It has been confirmed by the ^{2}HNMR and *PVT* studies that 50 - 60% of the transition entropy $(\Delta S_{tr})_p$ arises from the variation in the conformational distribution of the spacer at the phase boundary.[2,8]

The lowest energy state of n-alkane or polymethylene chains are the all-trans planar arrangement, which could be readily accommodated in the nematic environment. In contrast, polyoxyethylene (POE) is known as one of the most flexible polymers, and the chain crystallizes in a helical (7/2) arrangement. The OC-CO moiety of the POE chain prefers to take a gauche form in the unconstrained state. The purpose of the present work is to investigate the conformational characteristics of the OE spacer $-(OCH_2CH_2)_xO-$ under the influence of the nematic potential field. In the following, we report the nematic conformation of OE spacers revealed by the ^{2}HNMR analysis.

Experimental

Preparation of Samples

Twin compounds having various mesogenic units on both terminals of the OE spacers were prepared according to the scheme[11-13] listed below:

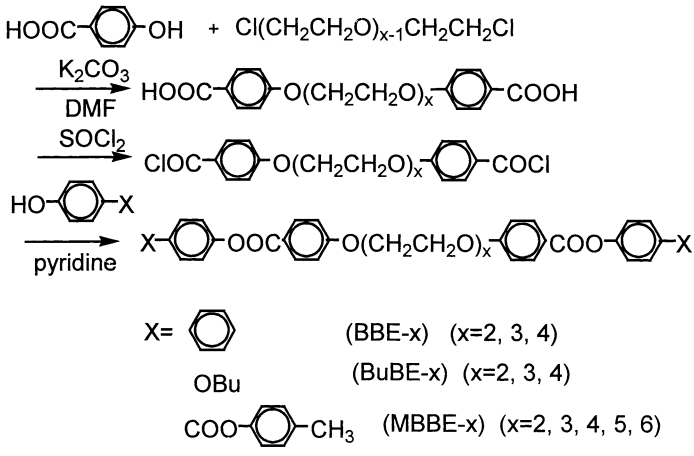

Abbreviated names of the compounds are indicated in parentheses: x denotes the number of OE units in the spacer.

Polymer samples having similar spacers were prepared by the conventional polycondensation method:[14-16]

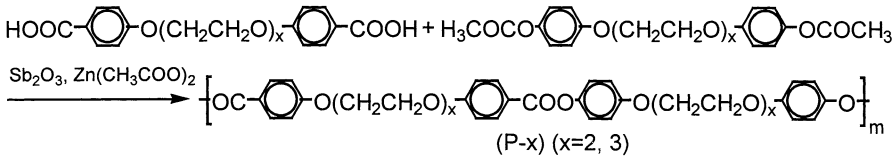

Polymers having partially deuterated spacers and mesogenic units were also prepared following the procedure described in the literature.[17-19] These polymer samples are hereafter represented by P-x.

Measurements

Thermal transitions were measured with a Perkin-Elmer differential scanning calorimeter (DSC) calibrated with indium. Heating rates of 10 deg min^{-1} were employed in most of the DSC scans. The phase transitions were observed by using an Olympus polarizing microscope equipped with a Mettler FP82 hot stage. The ^{2}HNMR spectra were recorded on a JEOL JNM-GSX-500 spectrometer operating at a 76.65 MHz deuterium resonance frequency. Measurements were carried out under a nonspinning mode. The molecular weights of polymer samples were obtained by gel permeation chromatography (GPC) with a SHOWDEX K-80M column using chloroform as the eluent: P-2, M_n=1.3x10^4, M_w=3.6x10^4;

P-3, M_n=3.0x10^3, M_w=1.1x10^4.

Results and Discussion

Thermal Analysis and Polarizing Microscope Observation of the Meso Phase

Phase transition temperatures and associated thermodynamic quantities obtained by using DSC are summarized in Table 1, where T_m, T_c, and T_{NI}, respectively, indicate the melting temperature of the crystal, the crystallization temperature, and the transition temperature from the isotropic to nematic phase. ΔH and ΔS are respectively the enthalpy and entropy changes at the phase transition as specified by the appended suffix, values being observed on heating unless otherwise noted. Most of the samples prepared exhibited meso phases, either enantiotropic or monotropic, the textures of the phase being identified as nematic under the polarizing microscope.

In consideration of the guaranteed temperature limit (200°C) of our standard ^{2}HNMR probe, BuBEs were chosen as the most appropriate dimer candidate to study the conformational characteristics of the OE spacer in the nematic state. With this reason, BuBE-x were extensively deuterated and used in the following analysis (see Table 1).

Table 1. Summary of DSC Data

	x	T_m	T_c	T_{NI}	ΔH_m	ΔH_{NI}	ΔS_m	ΔS_{NI}
		°C	°C	°C	kcal mol^{-1}	kcal mol^{-1}	cal mol^{-1} K^{-1}	cal mol^{-1} K^{-1}
BBE	2	188.9	169.0	191.9	18.1	0.59	39.2	1.28
	3	195.4	133.6	162.1[a]	17.9	0.62[a]	37.6	1.42[a]
	4	156.3	108.1	130.0[a]	14.8	0.23[a]	34.5	0.58[a]
BuBE	2	124.6	110.8	132.2	12.9	0.80	32.5	1.97
	3	99.0	68.9	103.0	12.6	0.76	33.8	2.03
	4	98.7	56.0	76.0[a]	13.5	0.54[a]	36.3	1.55[a]
MBBE	2	189.1	136.1	300.6	14.1	1.00	30.6	1.74
	3	163.9	121.3	271.0	13.3	0.95	30.5	1.75
	4	145.4	100.4	241.7	16.3	0.64	38.8	1.24
	5	127.9	91.9	215.5	6.1	0.28	15.3	0.58
	6	97.8	----	186.0	2.1	0.22	5.8	0.47
P	2	175.0	154.0	183.0[a]	----[b]	0.72[a,c]	----[b]	1.56[a,c]
	3	113.0	----	114.0[a]	----[b]	0.76[a,c]	----[b]	1.84[a,c]

[a]Estimated on cooling. [b]Values are not available due to an extensive overlap of the two endothermic peaks. [c]Expressed in terms of 'mol. of repeat unit'.

^{2}HNMR Observation

(1) BuBE-x (x = 2,3) and polymers in bulk

Examples of ^{2}HNMR spectra obtained for deuterated BuBE-x samples in the LC state are shown in Figs.1a and 2a. The deuterium atoms substituted on the aromatic cores of the mesogenic units exhibit splittings due to the dipolar couplings (D^{R}_{HD}) with the neighboring hydrogen in addition to the quadrupolar splittings ($\Delta\nu^{R}$). Here the values of $\Delta\nu$ and D_{HD} due to the mesogenic core are distinguished by the superscript R.

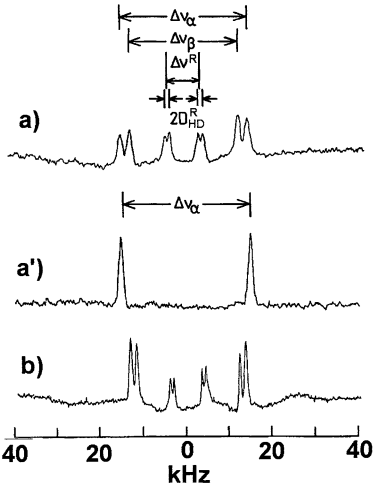

Figure 1. Examples of ^{2}HNMR spectra observed for (a) BuBE-2, (a') α-deuterated BuBE-2, and (b) BuBE-2 in PAA.

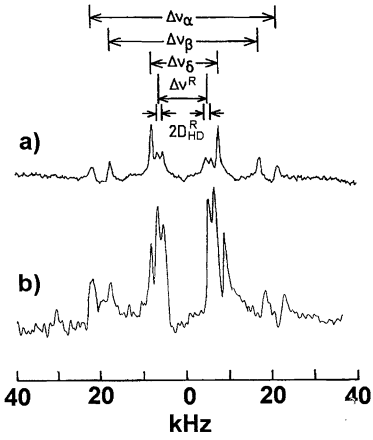

Figure 2. Examples of ^{2}HNMR spectra observed for BuBE-3 (a) in bulk and (b) in PAA.

Table 2. Observed Values of Quadrupolar and Dipolar Splittings for BuBE-x Samples in Bulk

Compound	T_r	$\Delta\nu^{R}$	$2D^{R}_{HD}$	$\Delta\nu_\alpha$	$\Delta\nu_\beta$	$\Delta\nu_\delta$
		kHz	kHz	kHz	kHz	kHz
BuBE-2	1.0	-7.13	-0.86	-27.97	-23.72	
	0.999	-7.10	-0.97	-27.65	-23.76	
	0.991	-9.09	-1.19	-34.60	-29.68	
	0.981	-10.21	-1.27	-38.04	-32.55	
	0.971	-10.86	-1.32	-40.75	-35.09	
BuBE-3	1.0	-8.96	-1.10	-35.13	-28.42	-12.43
	0.995	-10.36	-1.25	-39.70	-32.43	-14.28
	0.990	-11.26	-1.30	-45.53	-35.10	-15.48
	0.984	-11.89	-1.38	-45.39	-36.69	-16.31

For an unambiguous assignment of the peaks, a BuBE-2 sample deuterated specifically at the

α-position of the OE unit of the spacer was prepared. Comparison shown in Figs.1a and a' indicates that the outermost peaks originate from the α-CD bonds. In the ^{2}HNMR spectrum for the BuBE-3 sample (Fig.2a), the degree of deuteration helps to deduce a proper assignment: the deuterium content at the δ-position is about twice of that at the α-position along the spacer. The three doublet peaks of the spacer were thus identified as α, β, and δ in the order from the terminal carbon. Subscripts are appended to the individual $\Delta\nu$-values to distinguish the position of the CD bond along the chain. In Table 2, the observed values of quadrupolar and dipolar splittings are summarized, where the temperatures are expressed relative to that of the NI transition point: $T_r = T/T_{NI}$. At lower temperatures, the resonance peaks tend to be broader.

The present study has been extended to include polymers comprising the same spacers. As-made samples were adopted for the spectroscopic examination. The deuterium NMR studies were carried out for deuterated samples P-2 and P-3 (see Figs. 3a and 4a). While the

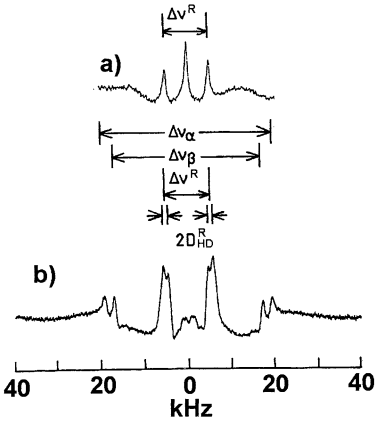

Figure 3. ^{2}HNMR spectra of (a)P-2 in bulk and (b) P-2 in PAA.

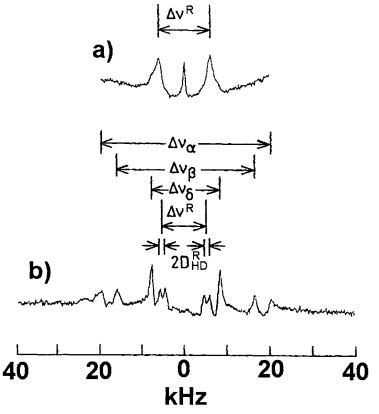

Figure 4. ^{2}HNMR spectra of (a) P-3 in bulk and (b) P-3 in PAA.

mesogenic cores exhibit broad resonance peaks, the signals from the CD bonds of the spacer are smeared out and almost indistinguishable. In all cases, the intensity of the central signals due to the isotropic fraction remains to be substantial throughout the LC state, indicating that the transformation to the nematic phase is incomplete. The origin of such an isotropic fraction is not clear at this moment. By judging from the molecular weight estimated by GPC, the samples should contain a sizable amount of low molecular weight fraction. The values of the observed $\Delta\nu^R$ are listed in Table 3.

Table 3. Observed Values of Quadrupolar Splittings for Mesogenic Cores of Polymers in Bulk

Compound	T_r	$\Delta\nu^R$
		kHz
P-2	1.0	-7.98
	0.992	-9.02
	0.982	-9.97
	0.974	-10.85
	0.964	-11.44
P-3	1.0	-11.09
	0.995	-11.92
	0.991	-11.94
	0.986	-12.27
	0.984	-12.50
	0.978	-12.05

Table 4. Observed Values of Quadrupolar and Dipolar Splittings for the Dimer and Polymer Samples in PAA

Compound	T_r	$\Delta\nu^R$	$2D_{HD}^R$	$\Delta\nu_\alpha$	$\Delta\nu_\beta$	$\Delta\nu_\delta$
		kHz	kHz	kHz	kHz	kHz
BuBE-2	1.0	-7.45	-0.88	-26.85	-24.07	
	0.999	-7.79	-1.00	-27.80	-24.97	
	0.994	-8.71	-1.04	-30.89	-27.74	
	0.986	-9.62	-1.10	-34.06	-30.39	
	0.979	-10.31	-1.20	-36.28	-32.25	
	0.969	-11.02	-1.26	-38.69	-34.30	
BuBE-3	1.0	-7.54	-0.95	-29.23	-23.69	-10.89
	0.998	-8.47	-0.97	-31.79	-26.02	-11.82
	0.993	-9.24	-1.16	-35.20	-28.39	-13.31
	0.988	-10.05	-1.21	-37.77	-30.25	-14.94
	0.980	-10.95	-1.24	-40.16	-32.69	-15.48
	0.968	-12.10	-1.36	-43.80	-36.08	-17.09
P-2	1.0	-10.01	-1.10	-37.94	-33.71	
	0.995	-10.45	-1.10	-38.64	-34.40	
	0.985	-10.92	-1.23	-40.70	-35.92	
	0.970	-11.61	-1.35	-43.63	-37.99	
P-3	1.0	-9.17	-1.18	-37.35	-29.54	-14.45
	0.995	-9.72	-1.20	-38.84	-30.71	-15.09
	0.990	-10.35	-1.19	-40.24	-32.42	-15.90
	0.982	-11.04	-1.20	-41.77	-33.86	-16.55

(2) Dimers and polymers hosted in a nematic solvent.

To obtain a better picture for the nematic conformation, P-x samples were dissolved in *p*-

azoxyanisole (PAA), which is a nematic low-molar-mass LC.[20] The ^{2}HNMR spectra obtained for a mixture containing 20wt.% P-x are included in the corresponding figures (see Figs.3b and 4b). From the phase diagram,[21] the eutectic composition of the mixture is estimated to be about 20-30wt.%. The temperature range (T_{NI}-T_c) of the nematic phase tends to be most expanded around this composition.

To facilitate comparison with polymers, the analysis was also carried out for the dimer sample BuBE-x dissolved in a nematic solvent, PAA. The spectrum obtained for a diluted sample (20wt.%) at T_r = 0.97 is shown in Figs.1b and 2b. The spectrum remains nearly identical irrespective of the dilution, suggesting that the conformation of the spacer is invariant as long as molecules are kept under the nematic field. The values of the observed splittings are summarized in Table 4.

Orientational Characteristics and the Nematic Conformation in the LC State

The order parameters of the mesogenic core axis were estimated from the observed D_{HD}^R and $\Delta\nu^R$ according to the procedure previously described.[22,23]

$$D_{HD}^R = -\gamma_H\gamma_D h/(4\pi^2 r_{HD}^3)S_{ZZ}^R \qquad (1)$$

$$\Delta\nu^R = (3/2)[S_{ZZ}^R \cdot q_{ZZ} + (1/3)(S_{XX}^R - S_{YY}^R)(q_{XX} - q_{YY})] \qquad (2)$$

Numerical values of the parameters required in these expressions were adopted from literature[22]: γ_H = 2.6752x10^8 kg^{-1}sA, γ_D = 4.1065x10^7 kg^{-1}sA, h = 6.6262x10^{-34} Js, r_{HD} = 2.48 A, q_{ZZ} = -18.45 kHz, q_{XX} = 113.85 kHz, and q_{YY} = -95.4kHz.

The order parameters S_{ZZ}^R and the associated biaxiality terms $S_{XX}^R - S_{YY}^R$ are tabulated in Tables 5 and 6. Since the splittings due to dipolar couplings D_{HD} could not be obtained for polymer samples in bulk, S_{ZZ}^R values were estimated from $\Delta\nu^R$, assuming that contribution of the $S_{XX}^R - S_{YY}^R$ term is comparable to that of the corresponding dimer LCs. The values obtained both in bulk and in the PAA solution are compared in these tables for given spacers. Although the actual phase transition temperatures T_{NI} are quite different between the bulk and solution, the ordering behaviors become quite similar when the temperature is expressed relative to T_{NI} (i.e., T_r). In all cases, the magnitude of the biaxiality term is small (<0.05) as is usually the case for the conventional nematic LCs.

In our previous studies,[3] the conformation of the spacer has been analyzed on the basis of the deuterium quadrupolar splitting data collected for the constituent CD bonds of the chain. In the RIS simulation scheme previously established,[3] the following expression was used for the

Table 5. Order Parameters for BuBE-2 and P-2 in Bulk and in PAA solution (20wt.%)

Compound	T_r	S_{ZZ}^R	$S_{XX}^R - S_{YY}^R$
BuBE-2	1.0	0.343	0.023
	0.999	0.396	0.037
	0.991	0.497	0.044
	0.981	0.517	0.039
	0.971	0.517	0.033
P-2	1.0	0.375	
	0.992	0.470	
	0.982	0.503	
	0.974	0.535	
	0.964	0.557	
BuBE-2/PAA	1.0	0.355	0.023
	0.999	0.403	0.032
	0.994	0.419	0.028
	0.986	0.444	0.025
	0.979	0.484	0.030
	0.969	0.508	0.029
P-2/PAA	1.0	0.444	0.022
	0.995	0.444	0.018
	0.985	0.496	0.027
	0.970	0.544	0.033

Table 6. Order Parameters for BuBE-3 and P-3 in Bulk and in PAA solution (20wt.%)

Compound	T_r	S_{ZZ}^R	$S_{XX}^R - S_{YY}^R$
BuBE-3	1.0	0.444	0.032
	0.995	0.505	0.034
	0.990	0.525	0.031
	0.984	0.557	0.034
P-3	1.0	0.521	
	0.995	0.555	
	0.991	0.556	
	0.986	0.568	
	0.984	0.576	
	0.978	0.560	
BuBE-3/PAA	1.0	0.383	0.029
	0.998	0.389	0.022
	0.993	0.468	0.035
	0.988	0.488	0.033
	0.980	0.498	0.027
	0.968	0.546	0.029
P-3/PAA	1.0	0.476	0.038
	0.995	0.484	0.035
	0.990	0.480	0.028
	0.982	0.484	0.023

deuterium quadrupolar splittings ($\Delta\nu_i$) of the spacer:

$$\Delta\nu_i = (3/2)(e^2qQ/h)S_{ZZ}\left(3\langle\cos^2\phi_i\rangle - 1\right)/2 \qquad (3)$$

where the quadrupolar coupling constant for the aliphatic CD bond is taken to be (e^2qQ/h) = 174 kHz.[24,25] Here we assume that the molecular axis (z) lies in the direction parallel to the line connecting the centers of the two neighboring mesogenic cores, and the molecules are approximately axially symmetric around the z-axis, and thus the orientation of these anisotropic molecules can be described by a single order parameter S_{ZZ}, the biaxiality of the system S_{XX} - S_{YY} being ignored for simplicity. In the equation above, ϕ_i is the angle between the ith CD bond and the molecular axis. The bracket indicates statistical mechanical averages taken over all allowed conformations in the system. In this model, the same value of S_{ZZ} is assumed to be applicable to all conformers in the mesophase. The order parameter S_{ZZ} may then be approximately related to S_{ZZ}^{R} of the mesogenic core by

$$S_{ZZ}^{R} = S_{ZZ}\left(3\langle\cos^2\psi\rangle - 1\right)/2 \qquad (4)$$

where ψ denotes the disorientation of the mesogenic core axis with respect to the molecular axis. The analysis of the experimental results may be facilitated by taking ratios such as

$$\Delta\nu_i/\Delta\nu^{R} = \text{Const}\cdot\left(3\langle\cos^2\phi_i\rangle - 1\right)/\left(3\langle\cos^2\psi\rangle - 1\right) \qquad (5)$$

or

$$\Delta\nu_i/\Delta\nu_j = \text{Const}\cdot\left(3\langle\cos^2\phi_i\rangle - 1\right)/\left(3\langle\cos^2\phi_j\rangle - 1\right) \quad (i \neq j) \qquad (6)$$

Here contribution from the biaxiality term to the observed $\Delta\nu^{R}$ is assumed to be negligible (cf. equation (2)). These ratios should solely depend on the spacer conformation, being free from the orientational order of the molecular axis S_{ZZ}.

The values of $\Delta\nu/\Delta\nu^{R}$ estimated for given temperatures (T_r) are plotted in Figs.5 and 6, respectively, for x=2 and 3. In these figures, the dimer and polymer carrying the same spacer are compared. For the dimer, the ratios obtained both in bulk and in the PAA solution are accommodated in the same figure. The values tend to decrease slightly with lowering temperature. The $\Delta\nu/\Delta\nu^{R}$ ratios fall nearly in the same range for given i's. Representative values taken from the figures are as follows: for spacers with x=2, $\Delta\nu_\alpha/\Delta\nu^{R}$=3.8, $\Delta\nu_\beta/\Delta\nu^{R}$=3.2; those for x=3, $\Delta\nu_\alpha/\Delta\nu^{R}$=3.9, $\Delta\nu_\beta/\Delta\nu^{R}$=3.1, $\Delta\nu_\delta/\Delta\nu^{R}$=1.4. These results immediately suggest that the conformational correlation along the spacer is controlled by the same principle throughout the nematic LC state (T_r = 1.0 ~ 0.97). It does not matter whether the spacer is a part of dimer or polymer. Since the flexible spacer maintains liquid-like

characteristics in the nematic state, the conformation of the spacer should be affected by the temperature, leading to a small variation in the ratio over a certain temperature range.

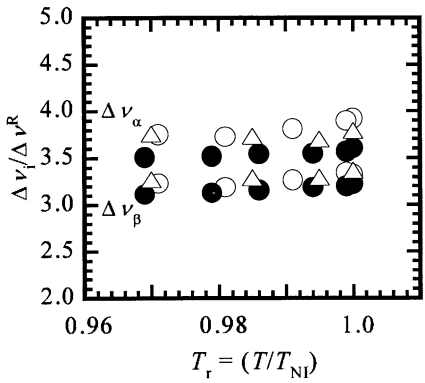

Figure 5. Quadrupolar splitting ratios $\Delta\nu_i/\Delta\nu^R$ plotted against temperature: BuBE-2 (open circles), BuBE-2 in PAA (filled circles), and P-2 in PAA (triangles).

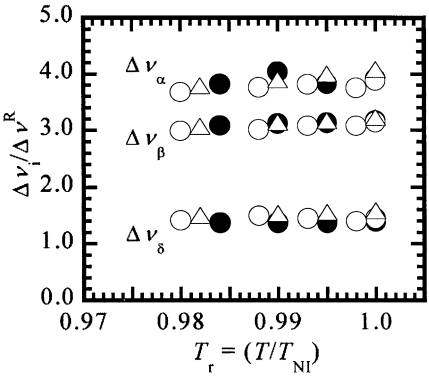

Figure 6. Quadrupolar splitting ratios $\Delta\nu_i/\Delta\nu^R$ plotted against temperature: BuBE-3 (open circles), BuBE-3 in PAA (filled circles), and P-3 in PAA (triangles).

Concluding Remarks

It is rather surprising to find that the ratios $\Delta\nu_i/\Delta\nu^R$ remain nearly invariant for given spacers independent of its origin: i.e., those from the dimer or polymer, or those observed in bulk or in the mixture with a nematic solvent. The same conclusion can be derived from the plots of $\Delta\nu_i/\Delta\nu_j$ vs. T_r constructed according to eq.6: the corresponding figures are omitted here to avoid redundancy. An ensemble of conformers characteristic to the nematic state may be termed the nematic conformation. These observations seem to confirm our previous conclusion derived from the analysis of a series of main-chain LC oligomers and polymers comprising n-alkane spacers. Elucidation of the individual conformers of OE spacers has however encountered some difficulty due to the fact that the number of adjustable parameters exceeds that collected from the ^{2}HNMR measurements. Further elaboration is needed.[26]

In the liquid crystalline state, the spacers should be allowed to take various conformations in as much as they are compatible with the preferred orientation of the mesogenic cores. Under these circumstances, the spacers are comparatively extended, and thus participate to some extent in the anisotropic intermolecular interactions in the nematic field.[27] While the orientation of the molecular axis (i.e., the whole molecule) varies sizably as a function of

temperature, the nematic conformation of the spacer is not much affected.

Some of the dimer compounds prepared in this study exhibit a nematic phase over a wider temperature range. These samples are well suited for the investigation of thermodynamic (*PVT*) properties of the nematic ensemble. Studies along this line are in progress.

[1] Abe, *Macromol. Symp.*, **1997**,*118*, 23.
[2] Abe, S. –Y. Nam, *Macromolecules*, **1995**, *28*, 90.
[3] Abe, H. Furuya, R. N. Shimizu, S. –Y. Nam, *Macromolecules*, **1995**, *28*, 96.
[4] Abe, H. Furuya, *Macromolecules*, **1989**, *22*, 2982; A. Abe, H. Furuya, *Mol. Cryst. Liq. Cryst.*, **1988**, *159*, 99; A. Abe, H. Furuya, D. Y. Yoon, *Mol. Cryst. Liq. Cryst.*, **1988**, *159*, 151.
[5] K. Inomata, Ph. D Thesis, Tokyo Institute of Technology, 1991.
[6] Abe, R. N. Shimizu, H. Furuya, "Ordering in Macromolecular Systems", A. Teramoto, M. Kobayashi, T. Norisuye, Ed., Springer, Berlin, 1994, 139.
[7] Y. Maeda, H. Furuya, A. Abe, *Liq. Cryst.*, **1996**, *21*, 365.
[8] Abe, T. Takeda, T. Hiejima, H. Furuya, *Polym. J.*, **1999**, *31*, 728.
[9] J. W. Emsley, G. R. Luckhurst, G. N. Shilstone, I. Sage, *Mol. Cryst. Liq. Cryst.*, **1984**, *102*, 223.
[10] Abe, *Macromolecules*, **1984**, *102*, 223.
[11] S. Tanimoto, R. Taniyasu, M. Okano, *Bull. Inst. Chem. Res., Kyoto Univ.*, **1978**, *56*, 340.
[12] J. –I. Jin, C. Ober, *Bull. Korean Chem. Soc.*, **1983**, *4*, 143.
[13] J. –I. Jin, Y. –S. Chung, J. –S. Kang, *Mol. Cryst. Liq. Cryst.*, **1982**, *82*, 261.
[14] L. Strzlecki, D. Van Luyen, *Eur. Polym. J.*, **1980**, *16*, 299.
[15] D. Van Luyen, L. Strzlecki, *Eur. Polym. J.*, **1980**, *16*, 303.
[16] W. Volksen, D. Y. Yoon, P. M. Cotts, *Macromolecules*, **1989**, *22*, 3846.
[17] T. Ishiguro, S. Kato, Y. Akazawa, *Yakugaku Zasshi*, **1943**, *63*, 282.
[18] G. B. Butler, Y. C. Chu, *J. Polym. Sci., Polym. Chem. Ed.*, **1979**, *17*, 859.
[19] S. Z. Perry, H. Hibbert, *Can. J. Res.*, **1936**, *14*, 77.
[20] F. Volino, M. M. Gauthier, A. M. Giroud-Godquin, R. B. Blumstein, *Macromolecules*, **1985**, *18*, 2620.
[21] T. Nakajima, Master Thesis, Tokyo Institute of Technology, 1991.
[22] J. W. Emsley, K. Hamilton, G. R. Luckhurst, F. Sundholm, B. A. Timimi, D. L. Turner, *Chem. Phys. Lett.*, **1984**, *104*, 136.
[23] N. Kimura, A. Abe, *Polym. Bull.*, **1992**, *28*, 81; A. Abe, N. Kimura, M. Nakamura, *Makromol. Chem., Theory Simul.*, **1992**, *1*, 401.
[24] S. Bruckner, J. C. Scott, D. Y. Yoon, A. C. Griffin, *Macromolecules*, **1985**, *18*, 2709.
[25] J. C. Rowell, W. D. Phillips, L. R. Melby, M. Panar, *J. Chem. Phys.*, **1965**, *43*, 3442.
[26] H. Iwanaga, Master Thesis, Tokyo Institute of Technology, 1990.
[27] H. Furuya, S. Okamoto, A. Abe, G. Petekidis, G. Fytas, *J. Phys. Chem.*, **1995**, *99*, 6483.